

ARTICLE

Semi-submersible Offshore Coupled Motion in Irregular Waves

Baoji Zhang* Ying Wang

College of Ocean Science and Engineering, Shanghai Maritime University, Shanghai, 201306, China

ARTICLE INFO

Article history

Received: 21 April 2020

Accepted: 1 June 2020

Published Online: 30 June 2020

Keywords:

Semi-submersible offshore platform

CFD method

Irregular waves

Motion response

Wave force

ABSTRACT

In order to predict the hydrodynamic performance of semi-submersible offshore platform accurately, based on CFD theory, continuous equation and N-S equation as the control equation, RNG type k- ϵ model as turbulence model, using the finite difference method to discretize the control equation, using the Semi-Implicit Method for Pressure Linked Equation (SIMPLE) algorithm to solve the control equation, using the VOF method to capture the free surface. The numerical wave tank of irregular wave is established, and the wave force and motion response of the semi-submersible platform under irregular wave are studied. Based on the Jonswap spectrum density function, for a certain area of two irregular waves (South China sea, a-ten-year return period, a-hundred-year return period) sea condition, five wave direction Angle (0°, 30°, 45°, 60°, 90°), a total of 10 kinds of conditions of the motion response of semi-submersible platform are simulated, through analysis and comparison of simulation results, the influence law of wave angle, wave period and wave height on platform motion is obtained. Compared with the experimental values, the results of heave and pitch are close to the experimental data under the sea condition of 2, 0 degree wave angles. The research results in this paper can provide reference for the design and motion response prediction of practical semi-submersible offshore platforms.

1. Introduction

How accurate and efficient use of computing resources, reappeared and verify that the classical theory, studying the problem that physical model experiments are difficult or even impossible to achieve, greatly reduce the computing cost, improve the calculation accuracy, is a important research topic in the field of hydrodynamics research, experts and scholars at home and abroad in recent decades of study, also has obtained many achievements. In foreign countries, Sarker^[1] considered the nonlinear stiffness of the anchorage system and the influence of interaction with fluid on the hydro-

dynamic of the platform, and introduced a new higher-order transfer function equation to analyze low-frequency surge, pitch and heave motions. Aidan^[2] uses the RANS method to simulate the diffraction and radiation problems of a single submerged spherical WEC during sway and surge. The linear finite element and CFD model of small wave amplitude are verified by the hydrodynamic coefficient of wave tank experiment. Then the nonlinear CFD model is extended to the larger amplitude model. Kim^[3] simulated vortex-induced vibration of TLP platform by using different CFD solving methods: Based on the finite element method, a flow field solver is used to simulate the sway and surge motions of TLP in the horizontal plane,

*Corresponding Author:

Baoji Zhang,

College of Ocean Science and Engineering, Shanghai Maritime University, Shanghai, 201306, China;

Email: zbj1979@163.com

and the six-degrees of freedom (6-DOF) motion of TLP is simulated by the boundary element method, and the numerical simulation results agree well with the model test results. Thanh-toan Tran^[4] provide an overview of the application and validation of CFD methods. The performance of the platform heave and pitch is studied by CFD method. The influence of unsteady aerodynamic performance of wind turbine rotor on the motion of the platform is proved. Luca^[5] based on the CFD method, and using the overlapping grid technology of the DFBI model contained in Star CCM+, simulates the platform motion and attenuation experiments under regular wave, and the simulation results are close to the experimental values. It also proves the practicability of the CFD method. Domestic scholars follow the forefront of research, Junlong Wang^[6] analyzed the semi-submersible platform related hydrodynamic theory and research methods, floating wave resistance, second-order wave, etc., compared the floating body motion analysis method in the frequency domain and time domain method, decoupling and decoupling analysis method, simple introduction of commonly used commercial software, the simplified analysis method of floating body motion is also discussed. Maoqiao Chen^[7] based on CFD software, the numerical simulation of two wave environments (regular wave and irregular wave) is carried out, and the influence of different wave angles and wave elements on the distribution of wave climbs is comprehensively analyzed. Yuanchuan Liu^[8] based on the Open source code (Open FOAM), the mooring system program was written, and the CFD method was used to analyze the movement performance of a floating wharf, and the high-nonlinearity phenomena such as wave-climbing and breaking occurred around the wharf. Wei Guo^[9] used CFD method to simulate and analyze the nonlinear stress characteristics of the hydrodynamic and dynamic output device PTO of a mooring double-floating wave energy device, the volume of fluid (VOF) method is used to simulate the wave formation and the floating body motion by combining the dynamic mesh with the rigid-body solution technique. The hydrodynamic and energy-receiving characteristics of a wave energy device under a nonlinear dynamic output device with different velocity indices are analyzed. Xu Wang^[10] based on the CFD method, a series of indoor experiments of solitary wave load were carried out on a semi-submersible platform using a double-layer plate-making wave machine. Combined with experimental results, a numerical tank of two-layer fluid based on N-S equation is developed to simulate the nonlinear interaction between ISW and semi-submersible platform. Zhining Bai^[11] in order to study the vortex-induced motion response of the deep semi-submersible platform, the experimental

study of the hydrostatic model was carried out, and the 6-DOF movement at different flow angles and different flow velocities were tested, and the motion time history, motion response amplitude, motion trajectory and so on were measured. The key problems of vortex-induced motion response of deep semi-submersible platform are analyzed. Fengqin Wang^[12] used the CFD method to calculate the resistance of the ship when the ship was trimming during the navigation, and verified the accuracy of the calculation results through the comparison of experimental values. All above proved the feasibility of the CFD method, and demonstrated the high practical value of the CFD technology.

It is concluded that with the rapid development of computer technology, the CFD method has been more mature, and the application of this method in the field of offshore engineering has achieved many achievements. The CFD method not only can effectively predict the wave force and motion response of floating structure in static water, but also can include wind, wave, flow and other environmental loads into consideration, and accurately predict the force and motion response of real scale floating structure under different sea conditions. In recent years, relevant studies at home and abroad show that: some researchers verify the feasibility of the relevant CFD method by comparing the numerical simulation with experimental values, at the same time, another part of the researchers directly applied the CFD method to the actual design and optimization, both of which have achieved a lot. With the application of more powerful large-scale computing workstations, the continuous improvement of information processing technology, the emergence of CFD commercial software, and the gradual improvement of turbulence model and computing method, the CFD method can definitely promote the progress and development of semi-submersible offshore platform. However, all the above scholars are studying the force and motion response of the semi-submersible platform under the regular wave, while actually the environment of the semi-submersible platform is random and irregular actual sea conditions. So it is more realistic to study the force and motion response of the offshore platform under the action of irregular waves. In this paper, on the basis of summarizing the predecessors' research results, based on the CFD technology research the force and motion response of the semi-submersible offshore platform in the irregular wave, based on the Jonswap spectrum density function, establish irregular wave numerical wave tank, research platform motion response in the irregular wave, analysis the influence law of its movement, its research results can provide technical support for the design of similar platform and useful reference.

2. CFD Basic Theory

2.1 Control Equation

The whole flow field uses the continuity equation and RANS equations as the governing equations ^[13]

$$\frac{\partial U_i}{\partial x_i} = 0, \tag{1}$$

$$\rho \frac{\partial U_i}{\partial t} + \rho U_j \frac{\partial U_i}{\partial x_j} = -\frac{\partial \hat{p}}{\partial x_i} + \frac{\partial}{\partial x_j} (\mu \frac{\partial U_i}{\partial x_j} - \overline{\rho u_i u_j}) + f_i^*, \tag{2}$$

where $U_i=(U,V,W)$ is the velocity component in the $x_i=(x, y, z)$ direction; ρ , \hat{p} , μ , $-\overline{\rho u_i u_j}$, and f_i^* are the fluid density, static pressure, fluid viscosity, Reynolds stresses, and body forces per unit volume, respectively.

2.2 Turbulence Model

The turbulence model adopts the renormalization group k-ε model, and the forms of the turbulence energy transport equation and energy dissipation transport equation are as follows ^[14]

$$\rho \frac{dk}{dt} = \frac{\partial}{\partial x_i} \left[(\alpha_k \mu_{eff}) \frac{\partial k}{\partial x_i} \right] + G_k + G_b - \rho \varepsilon - Y_M, \tag{3}$$

$$\rho \frac{d\varepsilon}{dt} = \frac{\partial}{\partial x_i} \left[(\alpha_\varepsilon \mu_{eff}) \frac{\partial \varepsilon}{\partial x_i} \right] + C_{1\varepsilon} \frac{\varepsilon}{k} (G_k + C_{3\varepsilon} G_b) - C_{2\varepsilon} \rho \frac{\varepsilon^2}{k}, \tag{4}$$

where μ_{eff} is the effective dynamic viscosity; and k and ε are the turbulent kinetic energy and turbulent dissipation rate, respectively. G_k is the generation of turbulent kinetic energy by the mean velocity gradients. G_b is the generation of turbulent kinetic energy by buoyancy. Y_M represents the contribution of the fluctuating dilatation to compressible turbulence. $C_{1\varepsilon}$, $C_{3\varepsilon}$, and $C_{2\varepsilon}$ are empirical constants.

2.3 Free Surface Capturing Method

The VOF method ^[15] is used to capture the free surface. This approach is a surface tracking method fixed under the Euler grid and simulates the multiphase flow model by solving the momentum equation and volume fraction of one or more fluids. The sum of the volume fractions of all the phases is one within each control volume. The equation of phase q is:

$$\frac{\partial \alpha_q}{\partial t} + \frac{\partial (u \alpha_q)}{\partial x} + \frac{\partial (v \alpha_q)}{\partial y} + \frac{\partial (w \alpha_q)}{\partial z} = 0, \tag{5}$$

where $q=0$ indicates that the unit is filled with water; $q=1$ represents that the unit is filled with air; α_0 and α_1 are the volume fractions of air and water, respectively; and $aq = 0.5$ is the interface of water and air.

2.4 Discretization and Solution of Equations

The commonly used numerical methods include finite volume, finite element, and finite difference methods ^[16]. The finite volume method is the intermediate product of the finite element and finite difference methods. Such method is also one of the widely used discrete methods in the field of CFD. In this study, the finite volume method is used to discretize the governing equations. A general form of the governing equations for 1D steady convection diffusion problems is as follows:

$$\frac{d(\rho u \varphi)}{dx} = \frac{d}{dx} (\Gamma \frac{d\varphi}{dx}) + 0, \tag{6}$$

where φ indicates the generalized variables and can be physical quantities to be sought for velocity and wave forces, Γ represents the generalized diffusion coefficient corresponding to φ , and S is the generalized source terms. In passive cases, $S=0$.

The central finite difference scheme is used to obtain the discrete equations.

$$\alpha_F \varphi_F = \alpha_W \varphi_W + \alpha_E \varphi_E \tag{7}$$

2.5 Establishment of a Numerical Wave Tank

2.5.1 Velocity Boundary Wave Making

Establishing a numerical wave tank with a wave-making function is a necessary condition for calculating the wave resistance of a ship. Numerical wave pools are mainly classified into two types: the first aims to imitate the wave-making physical method, and the other is pure numerical wave-making technology. Between these two types, the pure numerical wave-making technology is based on the CFD theory. The construction cost is low and the wave attenuation is slow. The ship speed can also be given at the entrance boundary; accordingly, the setting of the moving boundary in the physical wave-making method is avoided, and the computational complexity of the model is effectively reduced ^[17]. In this study, the setting wave-making boundary method is used to simulate the generation and propagation of linear regular waves.

The wave equation is

$$\eta = a \cos(kx - \omega_e t) \tag{8}$$

The velocity components in the horizontal and vertical directions are

$$u = a\omega_0 e^{kz} \cos(kx - \omega_e t) + U, \tag{9}$$

$$w = a\omega_0 e^{kz} \sin(kx - \omega_e t), \tag{10}$$

where k is the wave number determined by the formula $k = 2\pi / \lambda$, ω_0 is the natural frequency of the wave determined by the formula $\omega_0 = \sqrt{2\pi g / \lambda}$, ω_e is the encounter frequency of wave determined by the formula $\omega_e = \omega_0 + kU$, and U is the hull speed.

2.5.2 Numerical Wave Damping

The establishment of the damping region is necessary to prevent the influence of the reflected wave. The damping model provided by STAR-CCM⁺ is used to dampen the waves. The wave dissipation formula is deduced as follows: The length of the wave elimination region is generally one to two times the wavelength of the constant wave [18]. In this study, a damping term is added at the outlet of a numerical wave tank to ensure that the wave vertically attenuates and that the vertical velocity near the outlet of the numerical wave tank is almost zero. This task is conducted to eliminate the wave. The calculation formula is as follows [19]:

$$s_z^d = \rho(f_1 + f_2 |w|) \frac{e^{\kappa} - 1}{e^1 - 1} w, \tag{11}$$

where $\kappa = \left(\frac{x - x_{sd}}{x_{ed} - x_{sd}} \right)^{n_d}$ x_{sd} is the starting point of the

absorbing region; x_{ed} is the outlet boundary of the wave tank; f_1, f_2 , and n_d are the parameters of the model; and β is the vertical velocity component.

2.6 Six-DOF Motion Equation of Semi-submersible Aerodynamics

Two reference coordinate systems are created (Figure 1) while establishing the equation of motion of the semi-submersible floating foundation. The first is a coordinate system $O_0X_0Y_0Z_0$ fixed to the earth. The other is a moving system $GXYZ$ fixed to the semi-submersible floating foundation. The origin of the moving coordinate system is at the center of mass of the semi-submersible floating foundation. The equations of motions can be written as follows [20]:

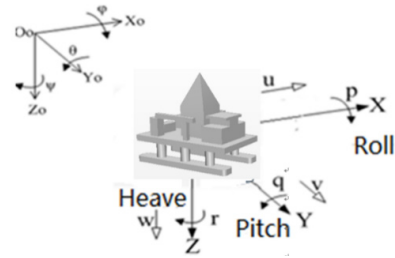


Figure 1. Fixed coordinates and coordinates with floating foundation

$$\frac{dB}{dt} + \Omega \times B = F \tag{12}$$

$$\frac{dK}{dt} + \Omega \times K + U \times B = M \tag{13}$$

where B is the momentum of the semi-submersible floating foundation, Ω is the angular velocity, F is the external force, K is the moment of momentum, U is the ship speed, and M is the resultant moment.

3. Irregular Waves

3.1 The Encounter Wave Energy Spectrum

In the study of the ship motions in waves, the frequency and the encountered frequency need to be converted. The encountered frequency depends on wave velocity, ship speed and wave propagation direction. Supposed that the ship is sailing in deep water, according to the relation of wave velocity in deep water, the encountered frequency can be converted as follows [21]. As shown in Fig 2.

$$\omega_e = \omega - \frac{\omega^2 U}{g} \cos \mu \tag{14}$$

Where, U is the ship speed, g is the gravity acceleration, ω is the wave frequency, μ is the encountering angle, quartering seas wave condition at $\mu = 135^\circ$, a heading wave condition at $\mu = 180^\circ$

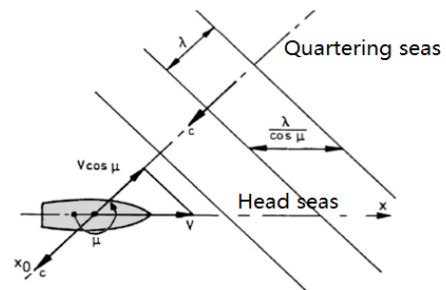


Figure 2. Encountering angle μ

For any reference systems, the total energy of waves is fixed. Therefore, the conversion of spectrum and encountered spectrum can be accomplished by the following formula:

$$m_0 = \int_0^\infty S(\omega) d\omega = \int_0^\infty S(\omega_e) d\omega_e \quad (15)$$

$$S(\omega_e) d\omega_e = S(\omega) d\omega \quad (16)$$

Also

$$\omega_e = \omega - \frac{\omega^2 U}{g} \cos \mu, \quad \frac{d\omega_e}{d\omega} = 1 - \frac{2\omega U}{g} \cos \mu$$

Therefore, the wave energy spectrum of the encountered frequency is:

$$S(\omega_e) = \frac{S(\omega)}{\left| 1 - \frac{2\omega U}{g} \cos \mu \right|} \quad (17)$$

The ITTC dual parameter spectrum is selected as the wave model and the wave characteristic periods and significant wave height must be input before the calculation. Fig3 shows the density curve of wave spectrum. The dotted line is the ITTC dual parameter spectrum about the frequency, and the solid line is the density curve of wave spectrum about the encountered frequency at different ship speeds. It can be seen from the figure, with the increasing of the speed, the position of the highest point reduces gradually, and the frequency value reaching the highest point increases gradually.

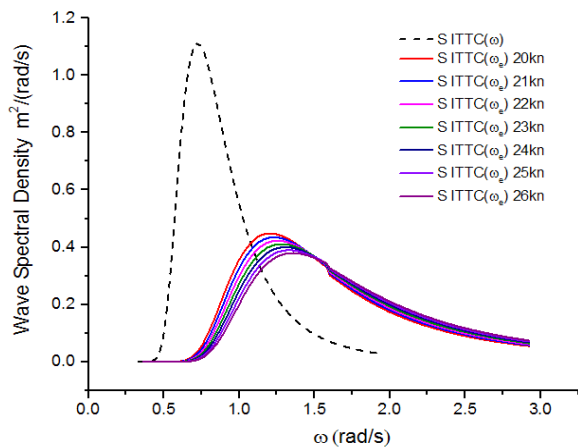


Figure 3. Curves of wave spectral density function at different speeds

3.2 Simulation Method

According to the classical wave model proposed by Longuet-Higgins et al. [22], the waves in a stationary sea state can be regarded as a stochastic process with steady states, and the fluctuation at a fixed position can be seen as a superposition of infinite amplitude, circle frequency and initial phase stochastic cosine wave. The wave surface expressions with fixed points are:

$$\eta(x, t) = \sum_{i=1}^N A_i \cos(k_i x - \omega_i t + \theta_i) \quad (18)$$

Where, N is the number of composition waves, k_i and ω_i is the wavenumber and angular frequency of the i -th component wave respectively, θ_i is the phase of the i -th constituent wave is uniformly and randomly distributed within $(0, 2\pi)$, A_i is the amplitude of the i -th component wave is expressed as:

$$A_i = \sqrt{2S_\eta \widehat{\omega}_i \Delta\omega_i} \quad (19)$$

Where, S_η is the spectrum of random waves, $\Delta\omega_i$ is the frequency interval, $\Delta\omega_i = (\omega_{i+1} - \omega_i) / i$, Lower limit of circular

Frequency $\omega_l = \frac{1}{5} \omega_p$, Upper limit of circular frequency $\omega_h = 5\omega_p$, ω_p is the spectral peak corresponds to the circular frequency, $\widehat{\omega}_i = (\omega_i + \omega_{i+1}) / 2$.

In the numerical simulation of irregular waves, the damping parameters of the numerical tank are different from those of regular waves. For the irregular wave generated in this paper, using the Jonswap spectrum, the damping length of the wave elimination area is about twice the wavelength corresponding to the peak frequency of the spectrum.

4. Numerical Example

4.1 Principal Dimensions and Parameters of Model

In this paper, the wave force and motion response of a semi-submerged offshore platform under irregular wave are simulated by CFD method, and the numerical simulation results are compared with the experimental values to verify the validity of this method. The model main scale and parameters of the semi-submersible offshore platform are shown in Table 1, and the three-dimensional geometric model of the platform is shown in Figure 4.

Table 1. Principal parameters of model

Type	Size	Type	Size
Length of semi-submerged platform (L)	111.6m	Offset column Height	18m
Width of semi-submerged platform (B)	66.4m	Offset column diameter	9.8m
Draft of semi-submerged platform (d)	16.5m	Platform mass	11.92E7kg
Length of float box	111.6m	Roll moment of inertia	88.08E11kg/m ²
Width of float box	18.8m	Pitch moment of inertia	11.30E11 kg/m ²
Height of float box	6.5m	Yaw moment of inertia	11.36E12 kg/m ²

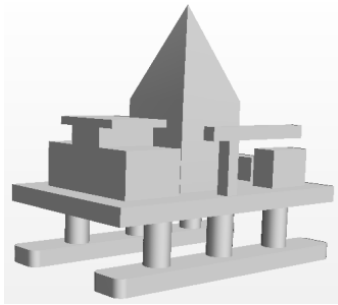


Figure 4. Geometric model of semi-submersible offshore platform

This study investigates the hydrodynamic performance of the semi-submerged offshore platform. Figure 5 shows the overall computing domain of the model. Considering the influence of wave length, the range of the x direction of the numerical wave tank is 600 m. Variable y should not be too short (ranging from -180 m to 180 m) to recede the wave reflection. The water depth is 250 m. Variable z is in the range of 200 m to -250 m. The lower part is water and the upper part is air. A damping region is set at the end of the computation domain to eliminate the effect of wave reflection on the calculation results at the exit. The length of this region is 120 m.

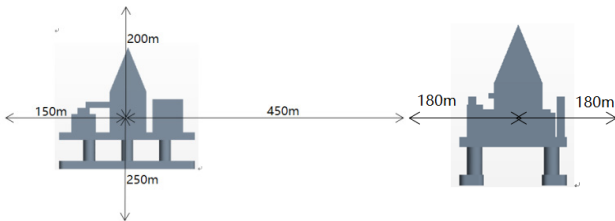


Figure 5. Calculation domain of model

4.2 Near Wall Modeling

The law of the wall is an empirically relationship for turbulent flows in close proximity to a wall. The log-law is only valid in the log-law region, which typically is $30 \leq y^+ \leq 200$ as seen in Figure 6. Further, it is seen that in

the viscous sublayer (i.e. $y^+ \leq 5$), the linear approximation ($u^+ = y^+$), while neither the linear nor the log-law holds in the buffer layer ($5 \leq y^+ \leq 30$).

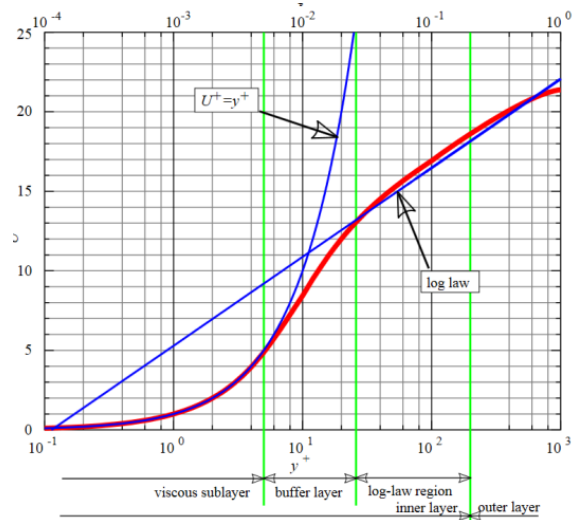


Figure 6. Law of the Wall [23]

To solve the turbulence problem in this work, we use the near wall model for the near-wall region of the ROV. The estimation of the first cell size y is based on the ITTC standard method and is given in the function of the non-dimensional wall distance y^+ and the local Reynolds number R_e of the ROV.

The expression for y^+ is

$$y^+ = \rho u_T \frac{y}{\mu}, \tag{20}$$

where u_T is the velocity friction defined as

$$u_T = \sqrt{\tau_w / \rho}$$

$$y = \frac{y^+ L}{R_e \sqrt{C_f / 2}}$$

$$C_f = \frac{0.075}{(\log_{10} R_e - 2)^2}$$

where L is the length of the ROV and C_f is the friction drag coefficient of the plate.

The y^+ variations of the offshore platform model for $U=1.0$ m/s are presented in Figure 7. The precision of the y^+ values of the offshore platform model determines the quality of the boundary layer solution that affects the friction force. The range of the y^+ values is $23 < y^+ < 700$.

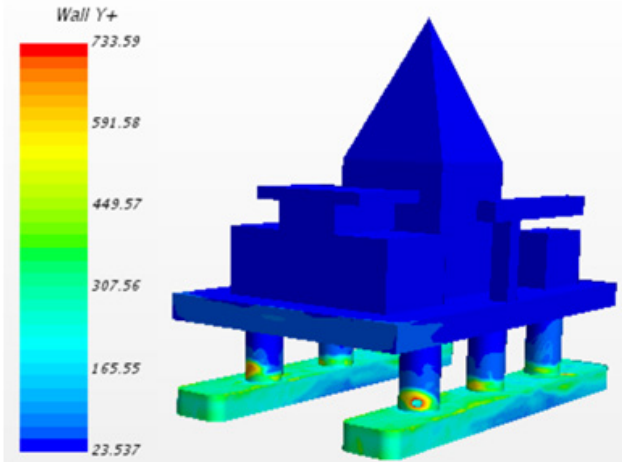


Figure 7. Wall y^+ of semi-submersible offshore platform

4.3 Meshing

The geometric model is imported into Star-CCM⁺, and the three-dimensional model is divided by the mesh technology of the Star-CCM⁺ software, and in the process of meshing, the effect of the fluid near the free surface on the offshore platform is more obvious. So the mesh close to the free surface should be denser, to ensure the number and quality of the mesh. Because the calculation model of this paper mainly carries on the vertical swinging and the longitudinal pitching simulation, and the gas and the fluid boundary flow field changes violently, here the grid should be denser. The size of the grid at the free surface depends on the free surface height, ensuring that 20 meshes are divided within the free surface height. If the free surface height is set to 5 m, the z-direction grid height is set to 0.25 m. In this case, the offshore platform is divided into 2.01 million grids, the overall grid division and boundary conditions as shown in Figure 8. The grid can be enlarged to save computational time, free-surface meshes and local grid as shown in Figure 9 and Figure 10.

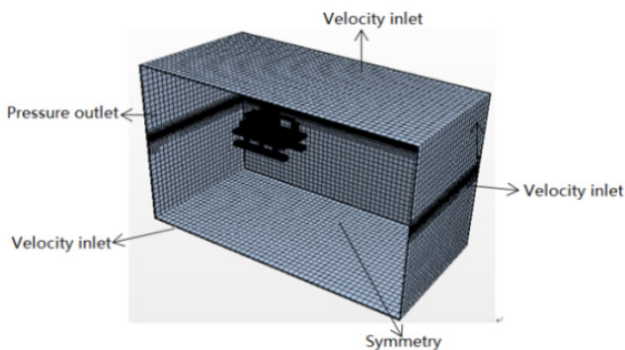


Figure 8. Boundary conditions of the model

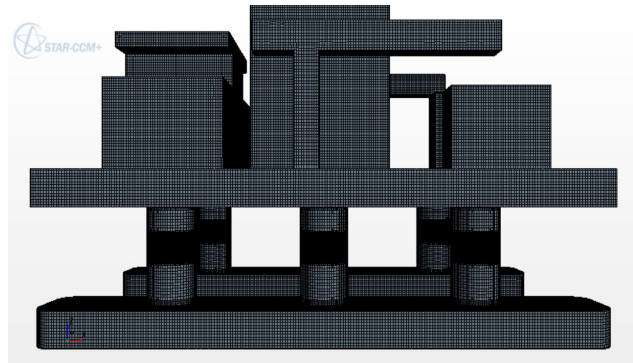


Figure 9. Grid of floating foundation

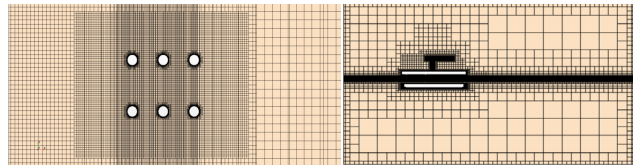


Figure 10. Free surface and section mesh of offshore platforms

4.4 Calculation Conditions

There are two kinds of random waves used in this study. According to bitner-gregersenem^[24] and the simulated random wave conditions, namely, the sea conditions of the south China sea that a-ten-year return period and a-hundred-year return period, the two kinds of sea condition parameters are shown in Table 6, wave angle refers to the Angle between the direction of the wave and the X-axis. Because the semi-submersible offshore platform deck below about X axial symmetry, so choose the waves to the five direction of 0° - 90°, respectively, as shown in Figure 11.

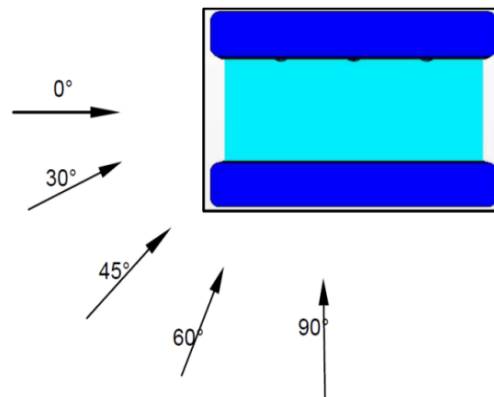


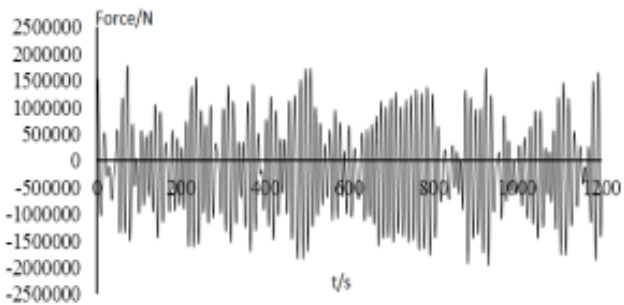
Figure 11. Wave direction of the semi-submersible offshore platform

Table 6. Sea condition parameters

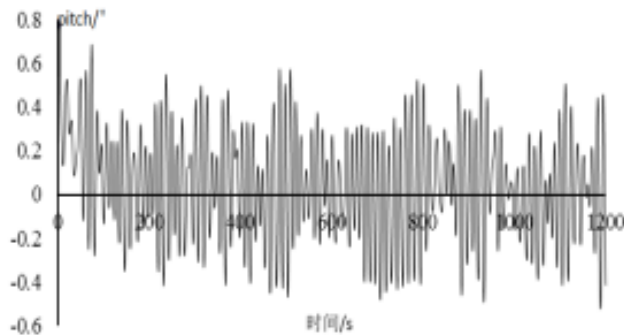
Sea Condition	γ	σ_a	σ_b	Significant wave height	Wave period	wave angle
Sea Condition 1 (a-ten-year return period)	3.3	0.07	0.09	6.2m	11.2s	0
	3.3	0.07	0.09			30
	3.3	0.07	0.09			45
	3.3	0.07	0.09			60
	3.3	0.07	0.09			90
Sea Condition 2(a-hundred-year return period)	3.3	0.07	0.09	10m	13.2s	0
	3.3	0.07	0.09			30
	3.3	0.07	0.09			45
	3.3	0.07	0.09			60
	3.3	0.07	0.09			90

4.5 Simulation Results and Analysis

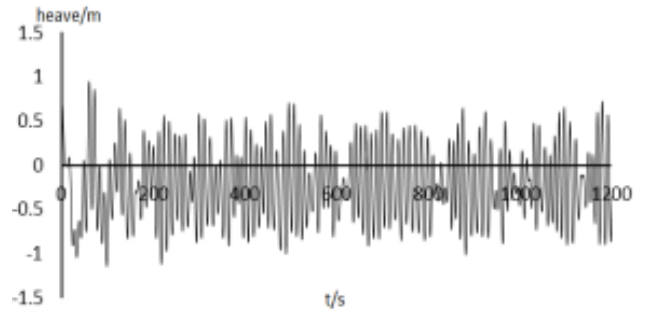
Sea conditions 1(a-ten-year return period), the simulated semi-submersible offshore platform in the draft 16.5m, there is a positive wave height of 6.2m, the wave period 11.2s conditions, different wave angle of the wave force. At 30°, the pitch and the heave response curve, as shown in Figure 12, the free surface waveform of the semi-submersible offshore platform in one cycle is shown in Figure 13.



(a) Wave force curve

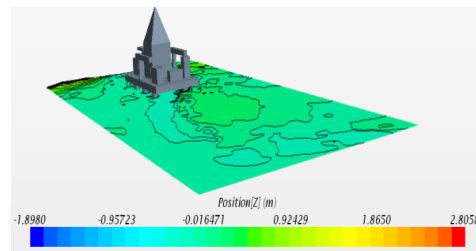


(b) Pitch response curve

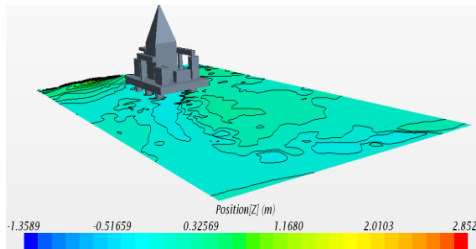


(c) Heave response curve

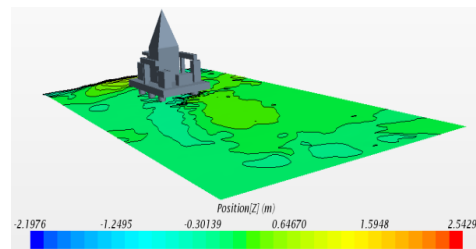
Figure 12. Motion response curve of a semi-submersible offshore platform at 30° wave angle



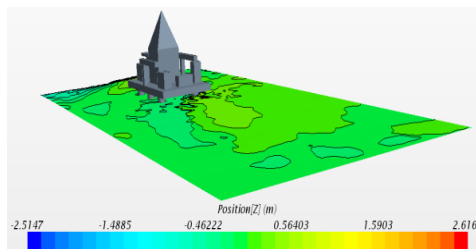
a) t=0.25T



b) t=0.5T



t=0.75T



t=1.0T

Figure 13. Sea Condition 1, Free surface waveform of semi-submersible offshore platform in one cycle at 30° wave angle

From the figure, the semi-submersible offshore platform in the Sea 1 (a-ten-year return period) by the Wave Force, the pitch and the heave is very complex and disorderly, the semi-submersible offshore platform by the wave force is irregular change, the range of the wave force in the -2.2×10^6 - 3.0×10^6 , the heave also shows irregular changes, The range of heave amplitude varies between -1.6m - 1.5m , and the pitch of the semi-submersible offshore platform is irregular, and the value of the pitch fluctuates between the -1.0° - 1.0° . The maximum wave force, pitch and heave are present in the case of a wave angle of 0 degrees, that is, under the heading condition.

Sea Condition 2 (a-hundred-year return period) simulated semi-submersible offshore platform in the draft 16.5m, there is a positive wave height of 10m, the wave period 13.2s conditions, different wave angle of the wave force. At 30° , the pitch and heave response curve, as shown in Figure 14, the free surface waveform of the semi-submersible offshore platform in one cycle is shown in Figure 15.

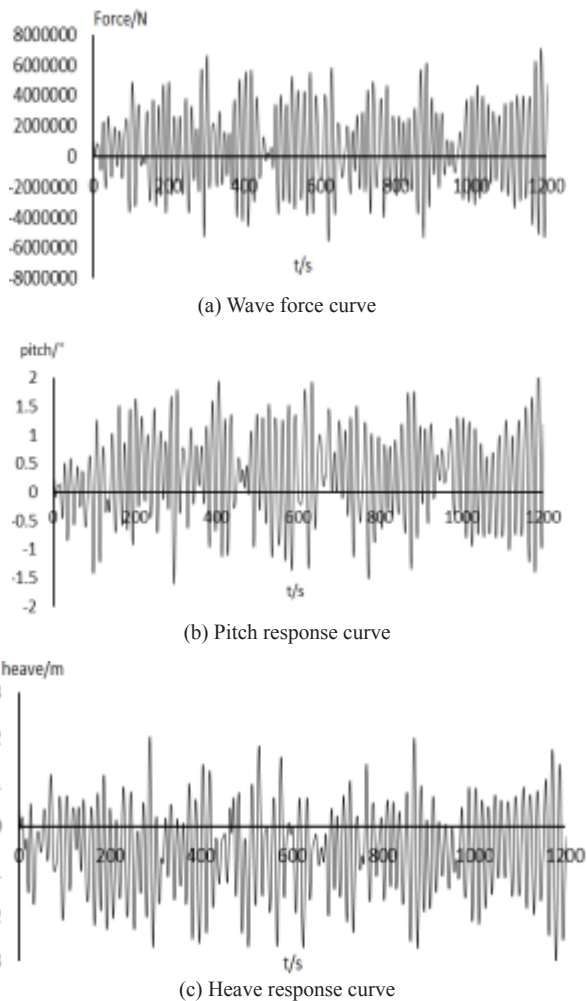


Figure 14. Motion response curve of a semi-submersible offshore platform at 30° wave angle

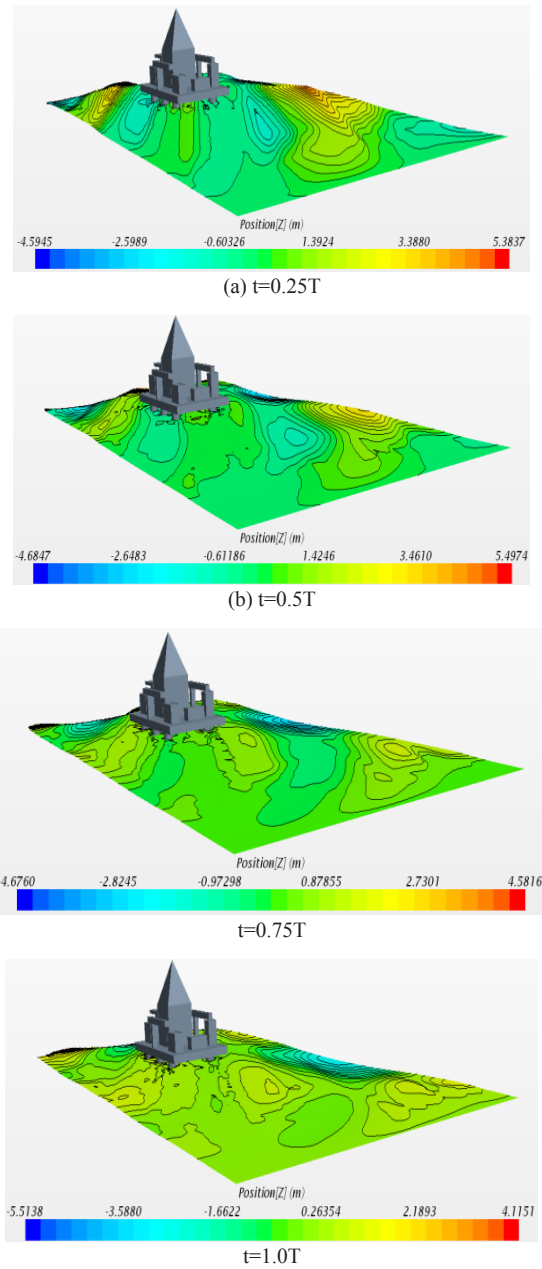


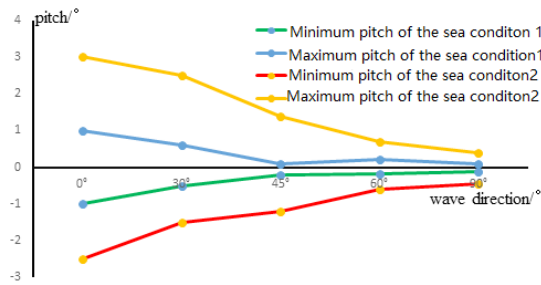
Figure 15. Free surface waveform of semi-submersible offshore platform in one cycle at 30° wave angle

It can be seen from the figure that under the condition of sea condition 2 (a-hundred-year return period), the wave force of the semi-submersible offshore platform is larger than that of sea condition 1, and the variation is very irregular, and the wave force range is between -6×10^6 - 9.0×10^6 . The heave and pitch motion are more intense, and the heave amplitude is larger, and the amplitude variation range is between -3.2m and 2.2m . Pitch is irregular, pitching angle between 2.5° and 3.0° , pitching angle of growth rapidly in a very short period of time to a lot of value. The main reason for this phenomenon is that

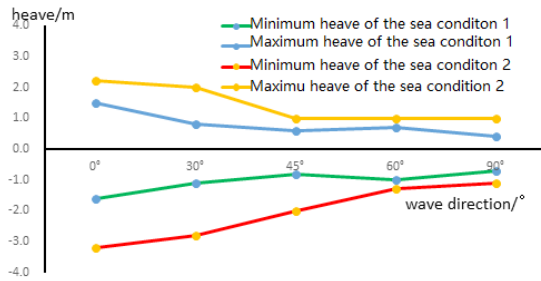
the wave of sea state 2 has significantly increased, and the wave height is the main parameter affecting the motion response of the semi-submersible offshore platform.

Table 7. Motion response and wave force summary of the semi-submersible offshore platform

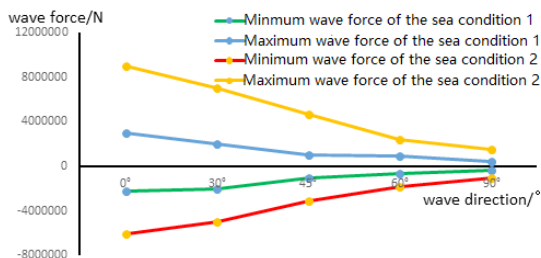
Sea Condition	Wave phase angle	Pitch (°)	Heave (m)	Wave force (N)
Sea Condition 1	0°	1.0	1.5	3×10^6
	30°	0.6	0.8	2×10^6
	45°	0.1	0.6	1×10^6
	60°	0.2	0.7	9×10^6
	90°	0.1	0.4	4×10^6
Sea Condition 2	0°	3.0	2.2	9×10^6
	30°	2.5	2.0	7×10^6
	45°	1.4	1.0	4.7×10^6
	60°	0.7	1.0	2.4×10^6
	90°	0.4	1.0	1.5×10^6
Sea Condition 2 (experiment value)	0°	2.56	2.5	-



(a) Pitch curve



(b) heave curve



(c) Wave force curve

Figure 16. Comparison of the values of heave, pitch and wave forces under irregular waves

It is shown from Figure 16 and Table 7 that the motion response and force of the platform under irregular wave

are very complicated and disordered, and the wave force and motion response of the offshore platform under different sea conditions have irregular changes. At 0° wave angle, the platform is most affected by the wave force, and the platform pitch and heave response is the most; at 90° angle, the platform has the least wave force, the platform pitch and heave response is the least; overall, with the increase of the wave angle, the platform pitch, heave and the wave force are gradually reduced. Under the same wave angle, the force and motion response of sea condition 1 and sea condition 2 can be found: the higher the period and the higher the wave height of the irregular wave, the greater the response of the platform to the wave force, the pitch and the heave. Compared with the experimental data, the results of heave and pitch are close to the experimental data under the sea condition of 2, 0 degree wave angles.

5. Conclusion

Based on the CFD method, the force and motion response of semi-submersible offshore platforms are studied, and the numerical wave tank of irregular waves is established. On the basis of the JONSWAP spectrum density function, the semi-submersible offshore platform under the irregular wave force and motion, corresponding to the simulation of the south China sea a-ten-year return period and a a-hundred-year return period two typical sea condition, five wave direction Angle (0°, 30°, 45°, 60°, 90°), a total of 10 kinds of working conditions of the motion response of semi-submersible offshore platform, it is concluded that the semi-submersible offshore platform pitching, heaving motion in the irregular wave is very complicated and disordered, And at the angle of 0° wave, the pitch is maximal, the angle of 90° wave, the pitch is the smallest.

Acknowledgments

Foundation item: National Natural Science Foundation of China (No. 51779135, 51009087), Shanghai Natural Science Foundation of China (project approval number: 14ZR1419500).

References

- [1] Sarkar A, Taylor R E. Low-frequency responses of nonlinearly moored vessels in random waves: coupled surge pitch and heave motions[J]. Journal of Fluids and Structures, 2001,15: 133-150.
- [2] Aidan Bharath, Jean-Roch Nader, Irene Peneis, Gregor Macfarlane. Nonlinear hydrodynamic effects on a generic spherical wave energy converter[J]. Renewable Energy, 2018, 118.

- [3] Tan J H C, Magee A, Kim J M, et al. CFD simulation for vortex induced motions of a multi-column floating platform [C]. Proceedings of the 32nd International Conference on Ocean, Offshore and Arctic Engineering. Nantes: OMAE, 2013: 11-17.
- [4] Thanh-ToanTran, Dong-Hyun Kim. The platform pitching motion of floating offshore wind turbine: A preliminary unsteady aerodynamic analysis[J]. Journal of Wind Engineering & Industrial Aerodynamics, 2015, 142.
- [5] Luca Oggiano, Fabio Pierella, Tor Anders Nygaard, Emile Arens. Comparison of Experiments and CFD Simulations of a Braceless Concrete Semi-submersible Platform[J]. Energy Procedia, Volume 94, September, 2016, 278-289.
- [6] Junrong Wang, Bin Xie. Review of Hydrodynamic performance and Global Motion Prediction of Semi- submersibles[J]. Shipbuilding of China, 2009, 50(Special): 255-260.
- [7] Maoqiao Chen. Study on climbing and near-field interference effect of deep-sea semi-submersible platform[D]. Jiangsu: Jiangsu University of Science and Technology, 2016.
- [8] Yuanchuan Liu. Numeical analysis of interaction of floating structures and mooring systems[D]. Shanghai: Shanghai Jiao Tong University, 2014.
- [9] Wei Guo, Nianfu Zhou, Shuqi Wang, Qiaosheng Zhao. Hydrodynamic and energy analysis of wave energy converter with nonlinear PTO[J]. Journal Huazhong University of Science and Technology(- Natural Science Edition), 2018, 46(4): 57-62.
- [10] Wang Xu, Jifu Zhou, Zhan Wang, Yunxiang You. A numerical and experimental study of internal solitary wave loads on semi-submersible platforms[J]. Ocean Engineering, 2018, 150(15): 298-308.
- [11] Zhining Bai, Longfei Xiao, Zhengshun Cheng, et al. Experimental study on Vortex Induced Motion response of a Deep Draft Semi-submersible platform[J]. Journal of Ship Mechanics, 2014, 18(4): 377-384.
- [12] Fengqin Wang. Study on calculation of floating resistance of ship longitudinal assembly based on CFD method[J]. Ship Science and Technology, 2017(22): 1-3.
- [13] P. Lin, P L F. Liu. A numerical study of breaking waves in the surf zone[J]. Journal of fluid mechanics, 1998, 24(3): 239-264.
- [14] Masoudian M, Pinho FT, Kim K, et al. A RANS model for heat transfer reduction in viscoelastic turbulent flow[J]. International Journal of Heat & Mass Transfer, 2016, 100: 332-346.
- [15] Shenglong Zhang, Baoji Zhang, Tahsin Tezdogan, Leping Xu, Yuyang Lai. Computational fluid dynamics based hull form optimization using approximation method, Engineering Applications of Computational Fluid Mechanics, 2017,12(3): 1-8.
- [16] Hirt C W, Nichols B D. Volume of fluid (VOF) method for the dynamics of free boundaries[J]. Journal of computational physics, 1981, 39(1): 201-225.
- [17] Shenglong Zhang, Baoji Zhang, Tahsin Tezdogan, Leping Xu, Yuyang Lai. Research on bulbous bow optimization based on the improved PSO algorithm, China Ocean Engineering, 2017, (33)4: 487- 494.
- [18] Peng Qi, Yongxue Wang. 3-D numerical-wave-tank technology and its application[J]. Journal of Dalian University of Technology, 2003, 43(6): 825-830.
- [19] Choi, Junwoo, Sung, Bum Yoon. Numerical simulations using momentum source wave-maker applied to RANS equation model[J]. Coastal Engineering, 2009, 56(10): 1043-1060.
- [20] Longo, J., Stern, F.. Uncertainty Assessment for Towing Tank Tests With Example for Surface Combatant DTMB Model 5415[J]. Journal of Ship research. 2005, 49(1): 55-68.
- [21] Baoji Zhang, Lei Niu. Study on Calculation Method of Added Resistance of Ships in Irregular Waves[J]. Naval Engineers Journal, 2017, 129(4): 123-134.
- [22] Longuet-Higgins M S. On an approximation to the limiting Stokes wave in deep water[J]. Wave Motion, 2008, 45(6): 770-775.
- [23] Peter Bradshaw, George P. Huang. The Law of the Wall in Turbulent Flow. Proceedings: Mathematical and Physical Sciences, Osborne Reynolds Centenary, 1995, 451(1941): 165-188.
- [24] Zehua Chen. Hydrodynamic performance analysis of semi-submersible platforms in extreme sea conditions[J]. China's water transport, 2018, 18(1): 16-18.